**Syntheses of Graphite Salts.** In our study different types of graphite starting material were used, i.e. spectrographic graphite (SG) and two kinds of pyrolytic graphite (PG), one from a graphite slab used for rocket nozzle cones, and the second one from highly oriented, mirror-surfaced graphite pieces. The pyrolytic graphites are more highly graphitized, better oriented, and more easily intercalated than the spectrographic graphite and, therefore, have been used almost exclusively in the previously reported studies.[11-13]

In agreement with the previous studies,[11-13] the reaction

$$nC + 0.5F_2 + BF_3 \rightarrow C_n^+BF_4^- \quad (5)$$

yielded a first-stage intercalate with $n$ being very close to 8.0 and the same identity period. No particular effort was made in this study to determine whether in $C_8BF_4$ the boron is present exclusively as $BF_4^-$ or if there might also be some free $BF_3$ and/or $F_2$ present.[13] It should be noted, however, that the addition of neat anhydrous HF to the (PG)- and (HOPG)$C_8BF_4$ generally resulted in gas evolution and a very pronounced swelling of the graphite salt, indicating the possible intercalation of some free $BF_3$.

For the synthesis of $C_n^+AsF_6^-$, the direct synthesis from graphite, $AsF_5$, and $F_2$ yielded for the two pyrolytic graphites $n$ values close to 9.8 and for spectrographic graphite a value of 11.6. With $O_2^+AsF_6^-$ used as the oxidant[14] and spectrographic graphite

$$nC + O_2^+AsF_6^- \rightarrow C_n^+AsF_6^- + O_2 \quad (6)$$

a composition of $C_{8.7}AsF_6$ was obtained. These salts were first-stage intercalates and approach the limiting composition $C_8AsF_6$, which has a close packing of the $AsF_6^-$ anions in the galleries.[18] For $C_nPF_6$, the direct synthesis using pyrolytic graphite, $PF_5$, and $F_2$ produced a first-stage intercalate having the composition $C_{12.4}PF_6$. The fact that the limiting composition for $C_nPF_6$ appears to be about $C_{12}PF_6$, while that for $C_nAsF_6$ is about $C_8AsF_6$, cannot be due to steric effects because $PF_6^-$ is smaller than $AsF_6^-$. It has been attributed[19] to the lower fluoride ion affinity of $PF_5$ relative to that of $AsF_5$. It, therefore, appears that $PF_6^-$ cannot support a positive charge on carbon higher than that corresponding to a composition of about $C_{12}^+$. Further evidence for the limiting composition of $C_nPF_6$ being about $n = 12$ was obtained by a displacement reaction between (PG)$C_{8.1}BF_4$ and liquid $PF_5$ at room temperature. Although only half of the $BF_3$ was displaced by $PF_5$ in a single treatment, the stoichiometry of the displacement reaction was such that 1 mol of $PF_5$ liberated 1.54 mol of $BF_3$; i.e., the $C_{8.1}BF_4$ was converted to $C_{12.5}PF_6$ and $BF_3$. The $C_{12.5}PF_6$ composition observed for this displacement reaction is in excellent agreement with that of $C_{12.4}PF_6$ derived from the direct synthesis from graphite, $PF_5$, and $F_2$ (see above). It is noteworthy that the stoichiometry of the above displacement reaction resembles that previously observed for the $C_7SO_3F + AsF_5$ system.[20]

In conclusion, our syntheses of graphite salts are in good agreement with the previous literature data suggesting limiting compositions of about $C_8BF_4$, $C_8AsF_6$, and $C_{12}PF_6$ for these first-stage intercalates.

**Ion-Exchange Reactions.** Solutions of $NF_4SbF_6$ in HF, when passed through columns of either $C_8BF_4$ or $C_8AsF_6$, readily exchange the $SbF_6^-$ anion for either $BF_4^-$ or $AsF_6^-$.

$$C_8BF_4 + NF_4SbF_6 \rightarrow C_8SbF_6 + NF_4BF_4 \quad (7)$$

$$C_8AsF_6 + NF_4SbF_6 \rightarrow C_8SbF_6 + NF_4AsF_6 \quad (8)$$

In this manner, spectroscopically pure $NF_4BF_4$ or $NF_4AsF_6$ can be prepared. It is important to use a suitable column geometry, i.e. a large height to diameter ratio, and a sufficient molar excess of the graphite salt. The importance of the column geometry and of flow conditions was demonstrated by an experiment whereby a sample of (PG)$C_{8.1}BF_4$ was stirred with a large excess of $NF_4SbF_6$ dissolved in HF. Even after a contact time of 10 h, only an insignificant anion exchange had occurred. The importance of using a sufficient excess of graphite salt over $NF_4SbF_6$ was demonstrated in an experiment where the mole ratio of $C_{8.7}AsF_6$ to $NF_4SbF_6$ was only 1.57. In this case the conversion of $NF_4SbF_6$ to $NF_4AsF_6$ was only 72 mol %.

Another important point is that the graphite salt starting material is fully oxidized to a $C_8^+$ stage. If the graphite salt is not completely oxidized, it will be oxidized by $NF_4SbF_6$ in a reaction, analogous to (6), resulting in the loss of $NF_4^+$ values.

$$8C + NF_4^+SbF_6^- \rightarrow C_8^+SbF_6^- + NF_3 + 0.5F_2 \quad (9)$$

This point was demonstrated in several experiments using $C_nBF_4$ compositions in which $n$ ranged from 14 to 16 and the yields of $NF_4BF_4$ were less than quantitative.

For the synthesis of $NF_4PF_6$, the most highly oxidized graphite $PF_6$ salt available was $C_{12.4}PF_6$. In view of the incomplete oxidation state of the graphite, it was not surprising that a 40 mol % loss of $NF_4^+$ values occurred during the exchange reaction.

**Conclusion.** Graphite salts can be used as anion-exchange resins that are highly resistant toward strong acids and oxidizers. To our knowledge, these are the first anion exchangers capable of withstanding such harsh conditions for which previously only cation exchangers, such as Nafion, were available. The usefulness of graphite salts as anion exchangers was demonstrated by an improved method for the production of advanced $NF_4^+$ salts. This method eliminates most of the drawbacks of the previously used low-temperature, metathetical process[6] and provides the desired $NF_4^+$ salts in high purities and yields by a simple, one-step process under ambient conditions.

**Acknowledgment.** We are indebted to Drs. C. J. Schack and W. W. Wilson for their help, to Dr. A. Moore for a sample of HOPG graphite, and to the Office of Naval Research and the U.S. Army Research Office for financial support.

Contribution from Ames Laboratory-DOE[1] and Department of Chemistry, Iowa State University, Ames, Iowa 50011

## Synthesis and Structure of the Zintl Phase $K_2SiAs_2$

Weir-Mirn Hurng, Eric S. Peterson, and John D. Corbett*

*Received April 14, 1989*

Binary, ternary, and higher compounds of the main-group elements afford a remarkable versatility in the compositions and structures that can be achieved in the so-called Zintl (valence) phases. The earliest considerations of this type of compound dealt with the close relationship perceived between the anions in these and the isosteric, isoelectronic units found for the elements. The parent member was NaTl in which $Tl^-$ in the diamond structure was thought to be analogous to, in particular, elemental Si, Ge, and (gray) Sn.[2] Further relationships of this sort included the very similar anion vs element structure connectivities and bonding in $CaSi_2 \triangleq As$, $NaSi \triangleq P_4$ and $NaSb \triangleq Te$.[3] Since then, many marvelous anionic networks, oligomers, and clusters have been discovered in which the same simple valence (octet) principles are operational but which cannot be realized in the structures of the

(18) Bartlett, N.; McQuillan, B. W. In *Intercalation Chemistry*; Wittingham, M. S., Jacobson, A. J., Eds.; Academic Press: New York, 1982.
(19) Hagiwara, R.; Lerner, M.; Bartlett, N. Presented at the ACS Ninth Winter Fluorine Conference, St. Petersburg, FL, Feb 1989; paper 63.
(20) Karunanithy, S.; Aubke, F. *J. Fluorine Chem.* **1984**, 25, 339.

(1) Ames Laboratory-DOE is operated for the U.S. Department of Energy by Iowa State University under Contract No. W-7405-Eng-82. This research was supported by the Office of Basic Energy Sciences, Materials Sciences Division.
(2) Zintl, E.; Woltersdorf, G. *Z. Elektrochem.* **1935**, *41*, 876.
(3) Klemm, W.; Busmann, E. *Z. Anorg. Allg. Chem.* **1963**, *319*, 297.

0020-1669/89/1328-4177$01.50/0 

elements or in binary compounds of the main-group metalloids and non-metals.[4]

We recently reported on one such example, $KSi_3As_3$, in which novel sheets had been formed by condensation of chains of rings of the non-metals.[5] In the course of this, we noted that small amounts of a possible $K_2SiAs_2$ were occasionally also obtained, the assignment being based solely on X-ray film studies of a single crystal that suggested the second phase was isostructural with $K_2SiP_2$.[6] We have subsequently refined single-crystal diffractometer data from this compound to confirm the earlier assessment and have since synthesized the phase in high yields. In the interim, a study of $Rb_2SiAs_2$ has also been reported.[7] We note here several new features, including a remarkable instability of $K_2SiAs_2$ and the fact that $K_2Si(As,P)_2$ and the binary phases $Si(Se,S)_2$[8] are not only isosteric but also isostructural except for the potassium cations.

## Experimental Section

**Synthesis.** Materials utilized were purified potassium (J. T. Baker Co.), which was trimmed of oxidation products in the glovebox, arsenic lumps (99.99% total, Alfa Products), and zone-refined, electronics-grade silicon. Loading of the reactants and examination of the products were carried out in gloveboxes which were flushed with nitrogen or argon plus helium. The moisture levels were below 3 ppm.

The original synthesis procedure for $K_2SiAs_2$ consisted of reaction of the appropriate quantities of the elements in fused silica containers at 800 °C[5] and gave only very low yields relative to $KSi_3As_3$, probably because of both the high temperature and a loss of potassium through reaction with the container. The previously developed two-step method for $KSi_3As_3$—preparation of KSi from the elements in tantalum at 800 °C followed by its reaction with more of the nonmetals in a silica container at ~910 °C—did not work well for $K_2SiAs_2$, the added potassium and arsenic presumably ending up in the container walls, which were colored bright red. However, large golden crystals of $K_2SiAs_2$ in 35–45% yields can be so achieved at 450–500 °C in 18–24 h.

A still better procedure is to first combine stoichiometric amounts of As and Si in a fused silica ampule under vacuum at 800 °C for 6 days to give $SiAs_2$. (The black powdered products also contain SiAs and ~10% As crystals.) A series of reactions were run in which stoichiometric amounts of ground $SiAs_2$ and potassium sealed within tantalum containers were slowly heated in a Marshall furnace to selected temperatures, held there for various time periods, and then furnace cooled. The best yield of $K_2SiAs_2$, ~70%, was obtained in three days at 450 °C, the remainder of the products being $KSi_3As_3$ as well as the elements and SiAs based on Guinier patterns. Less $K_2SiAs_2$ was obtained in the same period at higher temperatures or below 450 °C unless the reaction period is extended. A 5-week reaction at 450 °C gave only 20% $K_2SiAs_2$ and 80% $KSi_3As_3$ and simpler products.

*Caution!* $K_2SiAs_2$ may unexpectedly decompose at room temperature in the glovebox to give a sharp report, a brown cloud, and a shiny mirror. No shock wave has been noted under these conditions, presumably because the products are all solids. The explosive decomposition may initiate spontaneously or may occur on grinding or on contact with other objects, and it occurs more readily when the yield is 40% or greater, probably because of improved propagation. The reaction has occurred under $N_2$ or inert gas or when sealed in glass under vacuum. In the last circumstance, it can be initiated by a Tesla coil discharge or, when fairly pure, just by handling in which case a thick-walled Pyrex container was shattered. The weak and diffuse powder pattern obtained from the mirror appears to include Si, As and SiAs. The surface of the golden yellow crystals have also been observed to turn blue when pressure is applied, as with a spatula. No behavior of this character was mentioned for $Rb_2SiAs_2$.[7] The compound is also very sensitive to moist air in a more conventional hydrolysis/decomposition mode.

**Crystallography.** Single crystals of what turned out to be $K_2SiAs_2$ were mounted in 0.2-mm, thin-wall capillaries in the glovebox. Weissenberg photographs of the *hk*0 and *hkl* levels showed systematic absences $h + k + l \neq 2n$ for *hkl* and $h, k, l \neq 2n$ for *h*0*l* and 0*kl* reflections. Comparison of these and the provisional orthorhombic lattice constants with data in the literature suggested that the compound might be $K_2SiAs_2$, isostructural with $K_2SiP_2$,[6] with space group *Ibam* (appropriate to its instability).

Diffraction data were collected at room temperature on a crystal 0.04 × 0.04 × 0.75 mm with the aid of a four-circle DATEX diffractometer and graphite-monochromatized Mo K$\alpha$ radiation. Absorption was corrected for by applying a $\psi$-scan method. Programs for this, the subsequent refinement, mapping, and illustration have been referenced before.[9] Scattering factors used included the real and imaginary parts of anomalous dispersion.[10] The coordinates of $K_2SiP_2$ were used as input. The refinement was uneventful, and convergence at $R = 0.022$, $R_w = 0.026$ was obtained when anisotropic atom displacement parameters were introduced. The final difference Fourier map showed no residuals above ±1.0 e/Å$^3$.

Diffraction, refinement, and final positional parameters are collected in Table I, while more diffraction details, anisotropic atom displacement parameters, and structure factor data are available as supplementary material.

**Table I.** Diffraction, Refinement, and Positional Data for $K_2SiAs_2$

| | |
|---|---|
| space group, $Z$ | *Ibam* (No. 72); 4 |
| cell param ($a$, $b$, $c$),[a] Å | 13.132 (1), 6.999 (1), 6.340 (1) |
| $\mu$(Mo K$\alpha$), cm$^{-1}$ | 128.8 |
| range of transm coeff, normalized | 0.783–1.00 |
| struct soln:[b] $R$, $R_w$ | 0.022, 0.026 |
| atom positions ($x$, $y$, $z$; $B_{iso}$, Å$^2$) | |
| Si (222) | $^1/_2$, 0, $^1/_4$; 1.30 (7) |
| As ($m$) | 0.09880 (4), 0.33229 (9), 0; 1.62 (3) |
| K ($m$) | 0.3555 (1), 0.3383 (2), 0; 2.31 (6) |

[a] The cell dimensions calculated from Guinier powder diffraction pattern with Si as an internal standard, $\lambda = 1.540\,56$ Å. [b] $R = \sum||F_o| - |F_c||/\sum|F_o|$; $R_w = [\sum w(|F_o| - |F_c|)^2/\sum w|F_o|^2]^{1/2}$; $w = 1/\sigma_{F^2}$.

**Table II.** Important Distances (Å) and Angles (deg) in $K_2SiAs_2$[a]

| | | | |
|---|---|---|---|
| | Bonding Distances | | |
| Si–4As | 2.370 (1) | K–As$^{III}$ | 3.442 (2) |
| K–As$^{I}$ | 3.380 (2) | K–As$^{IV}$ | 3.497 (2) |
| K–2Si | 3.425 (1) | K–As$^{V}$ | 3.579 (2) |
| K–2As$^{II}$ | 3.435 (1) | | |
| | Nonbonding Distances | | |
| As–As | 3.527 (2)[b] | As–2As | 4.106 (1) |
| As–2As | 3.939 (1) | Si–2Si | 3.170 (0) |
| | Angles | | |
| As–Si–As | 96.14 (3)[b] | As–Si–As | 112.36 (4) |
| As–Si–As | 120.84 (4) | | |

[a] Roman superscripts on arsenic atoms refer to labels in Figures 2 and 3. [b] Shared edge.

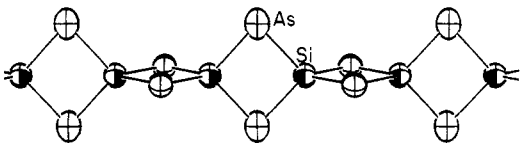


**Figure 1.** Portion of a $^1_\infty[SiAs_{4/2}^{-2}]$ chain in $K_2SiAs_2$, with silicon atoms shaded (95% probability thermal ellipsoids).

## Results and Discussion

Before considering the structural results, we should again call attention to the explosive decomposition often shown by $K_2SiAs_2$ at room temperature (see Experimental Section). Diminished yields from synthesis reactions run for a longer time at 450 °C or at higher temperatures strongly suggest that $K_2SiAs_2$ is only a kinetic intermediate on the way to $KSi_3As_3$ and binary phases. The stability difference is clearly greater near room temperature.

The compound $K_2SiAs_2$ contains parallel anionic chains of edge-sharing tetrahedra $^1_\infty[SiAs_{4/2}^{2-}]$ that are bridged both along and between the chains by potassium ions. The infinite chains lie parallel to $\vec{c}$ and form an approximately close-packed array when viewed along that axis (below). A side view of a portion of a single chain is given in Figure I, and important distances are

(4) Schäfer, H. *Ann. Rev. Mater. Sci.* **1985**, *15*, 1.
(5) Hurng, W.-M.; Corbett, J. D.; Wang, S.-L.; Jacobson, R. A. *Inorg. Chem.* **1987**, *26*, 2392.
(6) Eisenmann, B.; Somer, M. *Z. Naturforsch.* **1984**, *39B*, 736.
(7) Wolfe, J.; Weber, D.; von Schnering, H.-G. *Z. Naturforsch.* **1986**, *41B*, 731.
(8) Peters, J.; Krebs, B. *Acta Crystallogr., Sect. B* **1982**, *38*, 1270.
(9) Hwu, S.-J.; Corbett, J. D.; Poeppelmeier, K. R. *J. Solid State Chem.* **1985**, *37*, 43.
(10) *International Tables for X-Ray Crystallography*; Kynoch: Birmingham, England, 1974; Vol. IV, pp 72–146, 149–150.

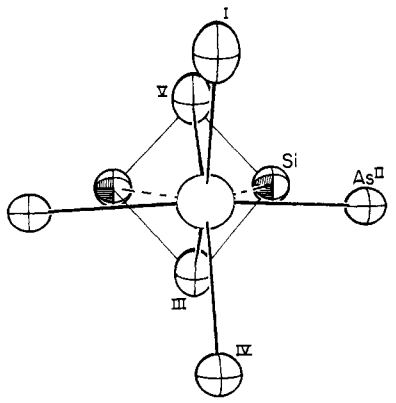


**Figure 2.** Environment of potassium (open ellipsoid) in $K_2SiAs_2$. The cation site is on a vertical mirror plane that lies approximately normal to the page and contains the shared edge of the $SiAs_4$ tetrahedra in the anion chain. The Roman numerals identify atoms with K–As distances in Table II.

listed in Table II. The single type of $SiAs_4$ tetrahedra in the chains have $D_2$ (222) point symmetry and are angularly distorted such that the shared (nonbonded) As–As edges of the tetrahedra, 3.53 Å, are 0.41 and 0.58 Å less than the other edges that have a component along the chain. This reflects a typical compromise in the internal angles in the Si–$As_2$–Si rhomboid about the shared edge (Figure 1) between those with an optimal tetrahedral bond angle at silicon and something close to 90° at arsenic, the results being 96.1 and 83.9°, respectively. These angles contrast with an average of 106.6° for ∠As–Si–As and 103.2° for ∠Si–As–Si for two-bonded arsenic in $KSi_3As_3$. The arsenic atoms in the latter occur in six-membered rings in which considerably less strain would be expected. We may also see the effect of strain in the Si–As distances in $K_2SiAs_2$, 2.370 (1) Å in the constrained linkage relative to 2.337 (2) Å for two-bonded arsenic in the more flexible ring system in $KSi_3As_3$. However, we note that their cation environments are also different (below).

A similar strained ring system and relatively larger Si–As distances are also found in $Ba_3Si_2As_4$.[11] The anion here consists of infinite chains constructed from –Si(As)$As_2$Si(As)– units in which four-membered Si–$As_2$–Si rings very similar to those in $K_2SiAs_2$ are interconnected through Si–Si bonds, there also being one terminal arsenic bonded to each silicon. The angles at arsenic are again a small and very similar 84.3°, while the Si–As bonds average a somewhat greater 2.406 (8) Å. Comparable Si–As distances and an Si–As–Si angle of 81° (error unspecified) are found in the strontium analogue according to a less thorough study.[12]

The role of the potassium in both sheathing the chains with cations and bonding them together is both novel and specific. The two-bonded arsenic in this compound bears a −1 formal charge and therefore exhibits stronger bonding with the cations. The very distorted octahedral environment of arsenic about a single potassium is shown in Figure 2, where the small Roman numerals key the atoms to distances listed in Table II. As viewed in the drawing, potassium lies on a mirror plane that is vertical and nearly normal to the page, and it is positioned almost directly above (and below) each rhomboid in Figure 1 (light outline) in such a way that it bridges both the arsenic atoms in the shared edge (III, V) and the closer pair of arsenic (II) atoms in adjoining bridges that are separated by the *b*-axis repeat. The two additional arsenic neighbors in Figure 2 that complete the distorted octahedral coordination lie toward the reader and occur in other chains, as will be considered below. The average K–As distance for the six contacts, 3.46 Å, corresponds closely to that between the four (of six) two-bonded arsenic neighbors in $KSi_3As_3$, 3.46 Å, and to that for seven at 3.47 Å in KAs[13] where the non-metal occurs in infinite

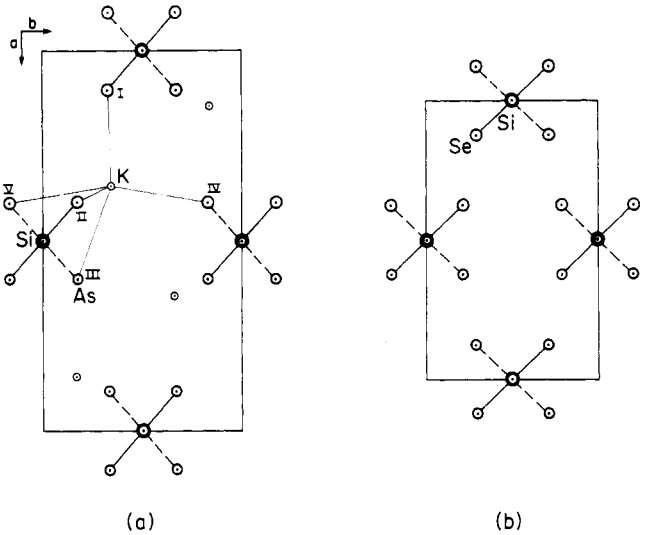


**Figure 3.** [001] sections of (a) $K_2SiAs_2$ and (b) $SiSe_2$.[8] Heavy circles are Si at $z = \pm 1/4$, with lighter circles representing As or Se at $\pm 1/4$ in $z$ from Si. The small circles mark only the K atoms at $z = 0$.

helical chains. The average distance between six-coordinate barium and two-bonded arsenic in $Ba_3Si_2As_4$, 3.40 Å, is consistent.

A striking feature of the potassium environment in $K_2SiAs_2$ is the presence of two silicon neighbors at 3.425 (1) Å, these interactions being designated by dashed lines in Figure 2. This separation appears to be significant alongside K–Si distances between $\mu_3$-K and $\mu_2$-K and $Si_4$ tetrahedra in $K_7Li(Si_4)_2$ and $K_3LiSi_4$ of 3.44 and 3.48 Å (average), respectively,[14] and an average of 3.35 Å to the silicon dodecahedra in the unusual $K_8Si_{46}$.[15] Presumably some of the negative charge on the $SiAs_2^{2-}$ chain in $K_2SiAs_2$ resides on the silicon atoms as well.

An unusual parallel also exists between $K_2SiAs_2$ and the isoelectronic $SiSe_2$[8] and, likewise, for the $K_2SiP_2$–$SiS_2$ pair, the parent structure types. The anion chains in the ternary phases are not only isosteric with those in the silicon dichalcogenides but they all occur in the same space group, *Ibam*. This is emphasized by the scaled [001] sections of $K_2SiAs_2$ and $SiSe_2$ shown in Figure 3 (the origin assigned[8] in the latter has been translated by $1/2$, 0, 0). The representation of the ternary compound on the left contains the silicon atoms lying at $z = \pm 1/4$ (heavy circles), the arsenic pairs in the surrounding tetrahedra that lie at $\pm 1/4$ in $z$ from silicon, and only the potassium ions at $z = 0$ (small circles). The K–As environment shown lies normal to that in Figure 2 and is again keyed according to distances in Table II.

The unusually simple relationships between the Zintl phases $SiSe_2$ and $K_2SiAs_2$ arise primarily because the selenium or arsenic atoms describe an approximately ccp array. Thus, the isosteric chains not only pack in the same way, but optimal potassium sites with the right multiplicity are also present on mirror planes at $z = 0$ and $1/2$ when the $SiSe_2$ lattice is simply expanded in *a* and *b*. Incidentally, the sequence has recently been extended with the discovery of $Na_3AlAs_2$.[16] In this case, the third cation is added to tetrahedral sites at 0, 0, $1/4$ and so forth.

Small distortions in the chains also appear to result from the introduction of the potassium cations into the $SiSe_2$ arrangement. Thus, the angles between planes that contain silicon as well as selenium or arsenic atoms in this projection, Figure 3, change slightly upon introduction of the potassium ions. The angle that is bisected by the *b* axis, which would be 90° with an $S_4$ operation along $\vec{c}$, increases from 86.5° in $SiSe_2$ to 96.3° in $K_2SiAs_2$ (96.9° in $Rb_2SiAs_2$), a change that appears to arise largely because of the K–$As^I$ interactions along $\vec{a}$.

There is also a somewhat surprising increase in Si–(Se,As) distances, from 2.275 (1) Å in the selenide to 2.370 (1) Å in the

(11) Eisenmann, B.; Jordon, H.; Schäfer, H. *Z. Naturforsch.* **1982**, *37B*, 1564.
(12) Eisenmann, B.; Schäfer, H. *Angew. Chem., Int. Ed. Engl.* **1980**, *19*, 490.
(13) Hönle, W. Ph.D. Thesis, Münster University, Münster, FRG, 1975.
(14) von Schnering, H.-G.; Schwarz, M.; Nesper, R. *Angew Chem.* **1986**, *98*, 558.
(15) Gallmeier, J.; Schäfer, H.; Weiss, A. *Z. Naturforsch.* **1969**, *24B*, 665.
(16) Cordier, G.; Ochmann, H. *Z. Naturforsch.* **1988**, *43B*, 1538.

ternary arsenide, whereas a difference of ~0.04 Å might be expected solely on the basis of the covalent radii.[17] This leaves one with the thought that introduction of charge into such isoelectronic systems, viz., for Si–Se → $Si-As^- K^+$, lengthens the Si–As bond appreciably. The same may occur when the higher field $Ba^{2+}$ is present in $Ba_3Si_2As_4$ (above) although the two types of arsenic atoms present there complicate the situation.

Previously, we were able to discern a concerted (but hypothetical) process of ring opening and bond formation whereby the structure of SiAs could be reductively converted to that of the anion sheet found in $KSi_3As_3$. This is not as direct for $K_2SiAs_2$ since the structure of the possible precursor $SiAs_2$[18] ($GeAs_2$ type[19]) includes As–As bonds in the five-membered rings that have been condensed into sheets.

**Acknowledgment.** Dr. W. Hönle kindly provided us with unpublished data on KAs.

**Registry No.** $K_2SiAs_2$, 108945-44-4; K, 7440-09-7; $SiAs_2$, 12255-97-9.

**Supplementary Material Available:** Tables of diffraction and refinement details and atomic thermal parameters for $K_2SiAs_2$ (2 pages); a listing of observed and calculated structure factor data (1 page). Ordering information is given on any current masthead page.

(17) Pauling, L. *The Nature of the Chemical Bond*, 3rd ed.; Cornell University Press: Ithaca, NY, 1960; p 225.

(18) Wadsten, T. *Acta Chem. Scand.* **1967**, *21*, 593.
(19) Bryden, J. H. *Acta Crystallogr.* **1962**, *15*, 167.

# Additions and Corrections

1988, Volume 27

**Karen Libson, Mary Noon Doyle, Rudy W. Thomas, Theodore Nelesnik, Mary Woods, James C. Sullivan, R. C. Elder, and Edward Deutsch***: Structural and Kinetic Investigations of a Tc(III)/Tc(II) Redox Couple. X-ray Crystal Structures of *trans*-$[Tc^{II}(DPPE)_2Cl_2]$ and *trans*-$[Tc^{III}(DPPE)_2Cl_2]NO_3 \cdot HNO_3$, Where DPPE = 1,2-Bis(diphenylphosphino)ethane.

Page 3615. In Table I the *y* coordinates of atoms C(34) and C(35) were incorrectly listed as positive numbers. The proper values are −0.0646 (4) for C(34) and −0.0255 (3) for C(35).—R. C. Elder